

A High Performance Uninterruptible Power Supply System with Power Factor Correction

R. Cáceres* N. Vázquez** C. Aguilar** J. Alvarez*** I. Barbi* J. Arau**

* Federal University of Santa Catarina
Power Electronics Institute
Florianópolis -SC- Brazil
Phone: 55-48-231-9204
Fax: 55-48-234-5422
E-Mail: ivo@inep.ufsc.br

** CENIDET
Electronics Engineering Dpt.
Cuernavaca, Mexico
Phone: 52 (731) 877-41
Fax: 52 (731) 224-34
E-Mail: cenidet1@infosel.net.mx

***CINVESTAV-IPN.
Electrical Engineering Dpt.
Mexico, D.F.
Phone: 52 (5) 747-7000
Fax: 52 (5) 747-7089
E-Mail: jalvarez@ctrl.cinvestav.mx

Abstract—In this paper a simplified sinusoidal uninterruptible power supply (UPS) system is presented. The proposed scheme includes features such as high power factor, low total harmonic distortion and good dynamic response on the output voltage. This scheme has the desirable features of high efficiency, simple circuit and low cost compared to a traditional standalone multiple stages UPS with power factor correction.

The circuit operation, analysis and experimental results of the proposed UPS scheme are presented. The UPS approach is a good solution for low power applications (≤ 500 W).

I. INTRODUCTION

To add an external UPS is the traditional approach used to provide uninterruptible power for applications such as personal computers, medical equipment, telecommunication systems, control systems, etc. On the other hand, it is desirable to include power factor correction (PFC) because of the well known advantages that this improvement represents. However, in order to get this capacity, it is necessary to add an extra power stage as we can see in Fig. 1.

Besides, the power inverter stage is done based on the full bridge buck inverter (FB-BI). In this case the output voltage is always lower than the DC input voltage, therefore it is necessary to add an extra stage to adequate its input voltage. There are two alternatives to achieve this objective:

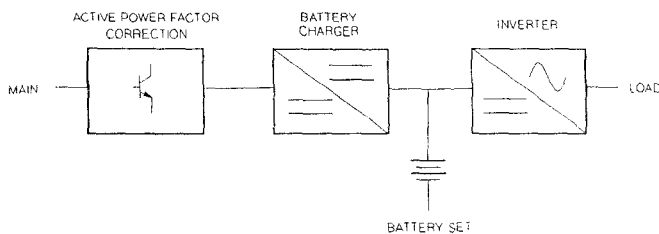


Fig. 1. Traditional uninterruptible power supply system with active PFC.

The first possibility is to build the inverter stage throughout the FB-BI and the boosting function by using a heavy and bulky low frequency transformer (Fig. 2a). The second possibility is to use a DC-DC boost converter in order to adequate the inverter input voltage (Fig. 2b).

The last option is more suitable due to benefits such as reduced size and low weight. The UPS using a two-stage PFC-battery charger and a two-stage high frequency DC link-inverter is shown in Fig. 3.

As it can be observed in Fig. 3, the UPS scheme consists of four power conversion stages resulting in poor efficiency, high cost and low reliability. In this paper, a novel scheme of an uninterruptible power supply system based on two power conversion stages is presented. The proposed configuration has high efficiency and low cost. Besides, it exhibits a close unity power factor.

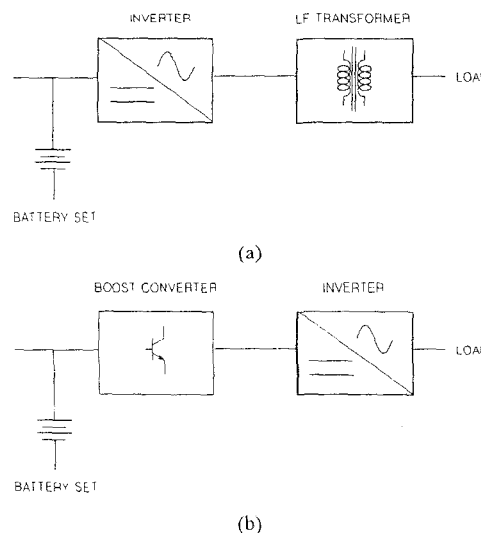


Fig. 2. Traditional alternatives to implement the inverter stage, (a) low frequency AC link, (b) high frequency DC link.

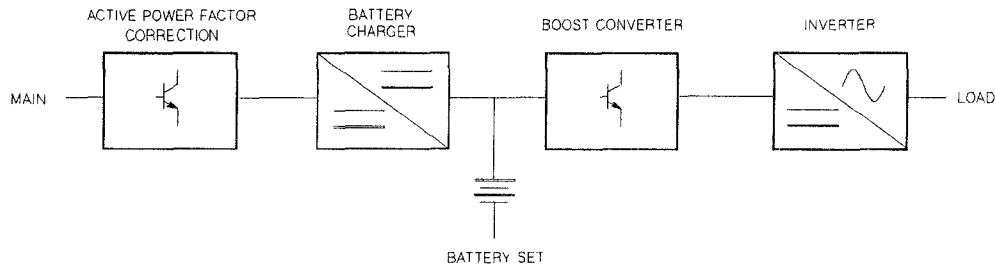


Fig. 3. Uninterruptible power supply system with active power factor correction and high frequency DC link.

II. PROPOSED SYSTEM

The proposed UPS based on two power conversion stages is shown in Fig. 4. The UPS offers excellent features, such as: simple structure, high power factor, low total harmonic distortion, fast dynamic response at the output voltage, high efficiency and low cost. These features make it a better solution than the classical approach.

The first stage of the proposed UPS consists of an integrated battery charger which was presented in [1]. This topology uses a discontinuous conduction mode (DCM) flyback converter in order to provide high power factor, battery charging, and high frequency isolation between both the main input and the battery set to the load. This structure does the functions of battery charging and power factor correction using just one magnetic structure, reducing the cost and accomplishing high reliability and simplicity of the converter. However, due to the use of the DCM flyback converter, it is suitable for low power applications (≤ 500 W).

The second stage is an integrated inverter topology with both boosting and inverting function. This topology was previously introduced in [2]. The boost DC - AC converter, referred to as *boost inverter*, features an excellent property: it naturally generates an output AC voltage lower or larger than the DC input voltage, depending on its duty cycle [2-4]. This property is not found in the classical voltage source inverter which produces an instantaneous AC output voltage always lower than the input DC voltage.

In the next paragraphs the operation principles of each stage of the proposed UPS structure will be described.

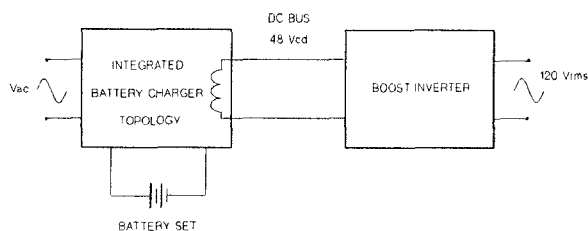


Fig. 4. Proposed uninterruptible power supply system.

III. BATTERY CHARGER-PFC STAGE

The basic circuit of the battery charger-PFC is shown in Fig. 5. As it can be seen in this figure, the converter can accept two input powers: one through the AC line and the other through the battery set. The topology has three operation modes [1]: normal mode, backup mode, and charging mode. The switch Q_1 controls the energy transfer in normal and charging operation mode, whereas Q_2 modulates the power transference when the converter operates in backup operation mode. The main converter (V_{AC} , L_1 and Q_1) operates when the main utility line is working properly, whereas the backup converter (V_{BAT} , L_2 and Q_2) operates when the principal energy supply fails. The switch Q_3 selects between the normal or backup operation mode and the charging operation mode. At the same time, it controls the battery charging current. In addition, the switch Q_3 protects the battery from high current levels that overpass the specifications of the battery manufacturer.

In normal and charging operation modes, the equivalent circuit of the integrated battery charger topology is a flyback converter operating in DCM. Therefore, it behaves in a natural way as a linear load to the utility line [5]. In backup operation mode the equivalent circuit is a well know DC-DC flyback converter. However, as the battery voltage is low, the peak and average current are higher than these ones in normal and charging operation mode. Therefore, we must be careful during the selection of the battery voltage bus.

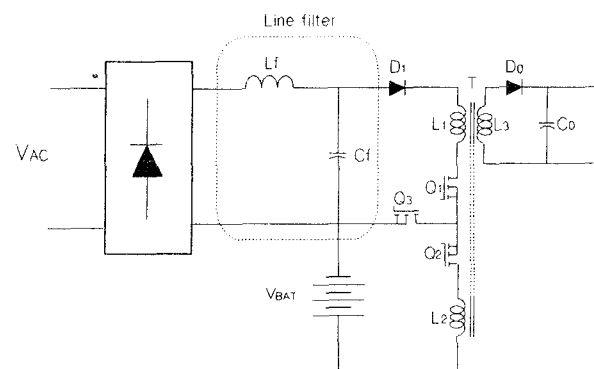


Fig. 5. Integrated battery charger topology as input stage of the proposed UPS.

In order to verify the battery charger-PFC stage, an experimental prototype was designed and built. The specifications were the following: output power = 250 watts, input voltage = 120 volts, $V_{BAT} = 48$ volts, and output voltage = 48 volts. The converter was implemented in DCM using a mixed device as power switch in order to increase the efficiency.

The experimental input voltage and current waveforms in normal operation mode are shown in Fig. 6. As we can see, the voltage and current waveforms are in phase. Therefore, a close to one power factor and low THD were obtained.

The converter was tested in charging operation mode too. The experimental input voltage and current waveforms are shown in Fig. 7 during this operation mode. As we can see in this figure, the input current waveform has a dead time crossing during the zero. This effect is due to the relatively high battery voltage bus [6], causing a reduction of the power factor and higher THD than those in normal operation mode. However, a higher V_{BAT} voltage means a higher efficiency in backup operation mode.

IV. BOOST INVERTER STAGE

The boost inverter achieves DC - AC conversion as follows: the power stage consists of two current bi-directional boost converter and the load is connected differentially across them (see Fig. 8). These converters produce a DC - biased sinusoidal waveform, so that each converter produces an unipolar voltage. The modulation of each converter is 180 degrees out of phase with respect to the other, which maximizes the voltage excursion over the load (Fig. 9).

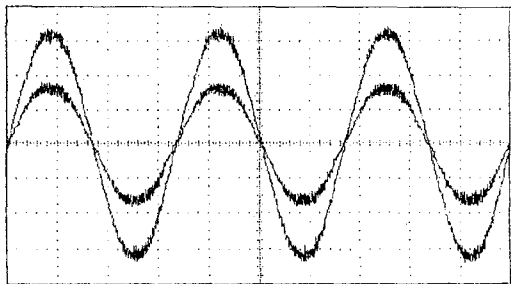


Fig. 6. Input voltage and current waveforms in normal operation mode.

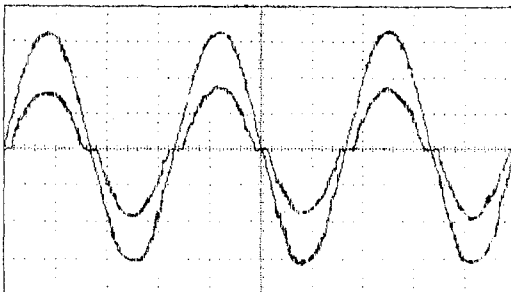


Fig. 7. Input voltage and current waveforms in charging operation mode.

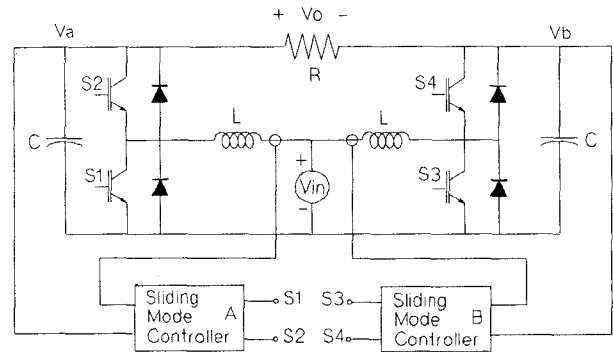


Fig. 8. Boost inverter with sliding mode control.

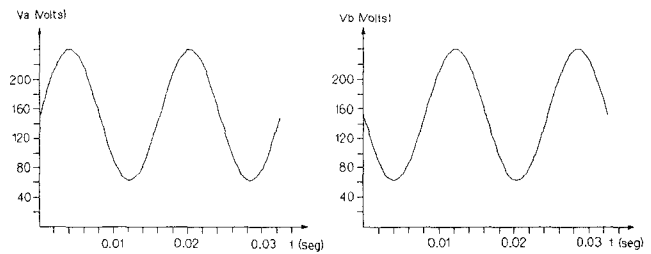


Fig 9. Output voltage for each DC-DC converter.

For the purpose of optimizing the boost inverter dynamics, while ensuring correct operation in any working condition, the sliding mode controller is one of the most suitable approaches. The main advantage, over the classical control schemes, is its robustness for plant parameter variations and invariant steady state responses in the ideal case.

A. System modeling.

Any DC-DC boost converter, which forms the boost inverter, could be substituted by a sinusoidal voltage source. On the other hand, there are two possible positions of the switch (-1 and 1). Taken into account these considerations, the simplified circuit of the boost inverter is the one shown in Fig. 10. The simplified circuit is modeled as a second order system.

The equations for each position of the switch are:

For $u = 1$:

$$\dot{x}_1 = b \tag{1}$$

$$\dot{x}_2 = c - w_1 x_2 \tag{2}$$

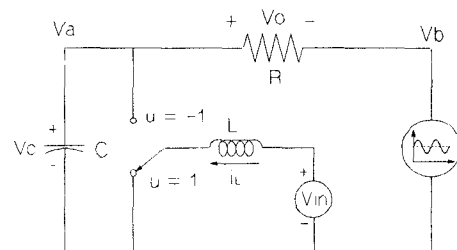


Fig. 10. Simplified circuit of the boost inverter.

For $u = -1$

$$\dot{x}_1 = b - w_0 x_2 \quad (3)$$

$$\dot{x}_2 = c - w_1 x_2 + w_0 x_1 \quad (4)$$

where

$$x_1 = I_r \sqrt{L}, \quad x_2 = V_c \sqrt{C}, \quad w_0 = \frac{1}{\sqrt{LC}}, \quad w_1 = \frac{1}{RC},$$

$$b = \frac{V_{in}}{\sqrt{L}}, \quad c = \frac{V_b}{R\sqrt{C}}$$

The system equations in matrix form are:

$$\begin{bmatrix} \dot{x}_1 \\ \dot{x}_2 \end{bmatrix} = \begin{bmatrix} 0 & -w_0/2 \\ w_0/2 & -w_1 \end{bmatrix} \begin{bmatrix} x_1 \\ x_2 \end{bmatrix} + \begin{bmatrix} 0 & w_0/2 \\ -w_0/2 & 0 \end{bmatrix} \begin{bmatrix} x_1 \\ x_2 \end{bmatrix} u + \begin{bmatrix} b \\ c \end{bmatrix} \quad (5)$$

$$\dot{\mathbf{X}} = \mathbf{A}\mathbf{X} + \mathbf{B}\mathbf{X}u + \mathbf{C} \quad (6)$$

B. Sliding controller design.

Sliding mode control offers advantages such as: stability, robustness, good dynamic response and simple implementation. However, the control theory involved is more complex than the traditional control theory.

Many papers have been presented a variety of sliding mode control design steps [7-11]. They could be summarized as follows:

- i) Propose the sliding surface.
- ii) Verify the existence of a sliding mode.
- iii) Analyze the stability in the sliding surface.

i) The sliding surface.

The sliding surface proposed is a lineal combination of the state variables and the reference variables, that is:

$$\sigma = \mathbf{S}\mathbf{X} - \mathbf{S}\mathbf{X}_r = \mathbf{S}\mathbf{e}\mathbf{X} \quad (7)$$

where:

$$\mathbf{S} = [s_1 \quad s_2],$$

\mathbf{X} = State variables,

\mathbf{X}_r = Reference variables.

$$\mathbf{e}\mathbf{X} = [ex_1 \quad ex_2]^T$$

The control law proposed is:

$$u = u_{eq} + u_N \quad (8)$$

where:

$$u_{eq} = \text{Equivalent control}$$

$$u_N = -\text{sgn}\sigma$$

This control law is composed by two terms, the first is only valid on the sliding surface (u_{eq}) and the other assures the existence of a sliding mode.

ii) Existence of a sliding mode.

Existence of a sliding mode implies that the following condition is fulfilled [7]:

$$\sigma \dot{\sigma} < 0, \quad (9)$$

resolving for $\dot{\sigma}$:

$$\dot{\sigma} = \mathbf{S}[\mathbf{A}\mathbf{X} + \mathbf{B}\mathbf{X}u_{eq} + \mathbf{C} - \dot{\mathbf{X}}_r] + \mathbf{S}\mathbf{B}\mathbf{X}u_N \quad (10)$$

Therefore

$$\sigma \dot{\sigma} = \mathbf{S}\mathbf{B}\mathbf{X}[-\sigma \text{sgn}\sigma] < 0 \quad (11)$$

In order to guarantee the existence conditions of a sliding mode the following inequality must be fulfilled:

$$\mathbf{S}\mathbf{B}\mathbf{X} > 0 \quad (12)$$

or

$$s_1 x_2 - s_2 x_1 > 0 \quad (13)$$

In order to assure the existence conditions, s_1 must be positive (due to x_2 is always positive) and greater than the absolute value of s_2 .

iii) Stability analysis in the sliding surface.

A tool developed to describe the movement in the sliding surface is the equivalent control [12]. The equivalent control is applied when $\sigma = 0$, hence $\dot{\sigma} = 0$. These conditions imply that the system is in the sliding surface.

Equivalent control (u_{eq}) is obtained from $\dot{\sigma} = 0$, therefore:

$$u_{eq} = -[\mathbf{S}\mathbf{B}\mathbf{X}]^{-1}[\mathbf{S}\mathbf{A}\mathbf{X} + \mathbf{S}\mathbf{C} - \mathbf{S}\dot{\mathbf{X}}_r] \quad (14)$$

The condition $\mathbf{S}\mathbf{B}\mathbf{X} \neq 0$ must be satisfied to avoid singularities in the equivalent control.

The equivalent control is substituted in the model of the system, and if the system eigenvalues have a negative real part, the system is stable.

C. Simulations results.

The system has been simulated with the following parameters: $L=0.36$ mH, $C=30\mu\text{F}$, $R=32.4\Omega$, $V_{in} = 50$ Volts, $V_o = 180$ Vac, $f = 60$ Hz.

Simulation results with $s_1 = 3$ and $s_2 = 1$ show the existence of a sliding mode, but the system has a slow response (see Fig. 11). In the phase plane graph it is shown that the system reaches the sliding surface and it is maintained there.

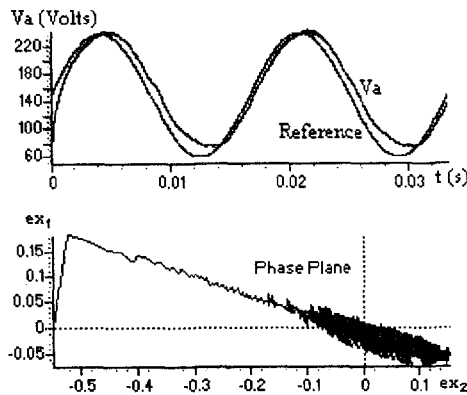


Fig. 11. Simulated results with the parameters $s_1 = 3$ and $s_2 = 1$.

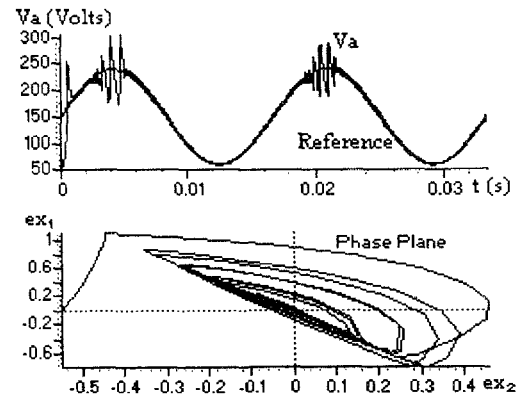


Fig. 13. Simulations with $s_1 = 0.4$ and $s_2 = 1$.

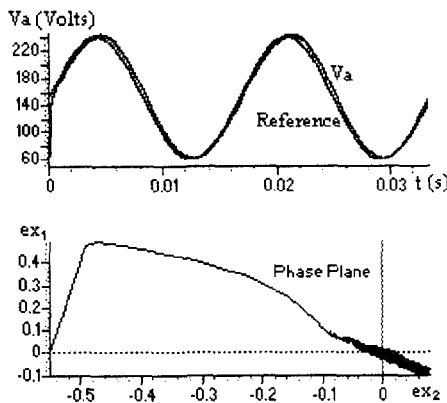


Fig. 12. Simulations with $s_1 = 1$ and $s_2 = 1$.

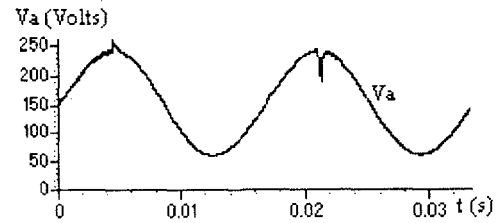


Fig. 14. Simulation with load variation. $s_1 = 0.8$ y $s_2 = 1$.

Also, the system has been simulated with the parameters $s_1 = 1$ and $s_2 = 1$ that demonstrate that if s_1 becomes lower by maintaining s_2 constant, the system is faster, as we can see in Fig. 12. In the phase plane graph it is shown that the existence is fulfilled in steady state, but it does not in transient operation. However even the existence condition is not fulfilled in the transient operation the system is stable.

A simulation with $s_1 = 0.4$ and $s_2 = 1$ demonstrates that if s_1 becomes too low by maintaining s_2 constant there is no a sliding mode even in the steady state (Fig. 13). A phase plane graph show that the existence is not fulfilled. It is important to note that when the system stays in the sliding surface the system dynamics is the fastest.

A simulation with a load variation was done in which the load has changed from $R=32.4$ to $R=1000$, and vice versa (figure 14). This simulation demonstrates the fast dynamics and robustness of the system by using the sliding mode control.

As it can be seen in the simulations made, there is a strong compromise between the existence condition and the fastness of the system.

D. Experimental results.

In order to validate the proposed idea, a 250 W prototype of the boost inverter was implemented. The following parameters were adopted:

$L = 360 \mu\text{H}$, $C = 32 \mu\text{F}$, $P_o = 250 \text{ W}$, $V_{in} = 48 \text{ V}$, $V_o = 120 \text{ Vac}$, $f_o = 60 \text{ Hz}$, $f_{s \text{ max}} = 30 \text{ kHz}$.

The inverter output voltage waveform, operating at no load, is shown in Fig. 15. The total harmonic distortion under this load condition is 1.2 %. Fig. 16 shows the inverter output voltage and current waveforms for a resistive load corresponding to 250 W. The instantaneous AC voltage is 170 V, which means a rms value equal to 120 V. The total harmonic distortion under this load condition is 1.78 %. As we can see, the sliding mode controller is a good alternative to achieve low THD for any load condition.

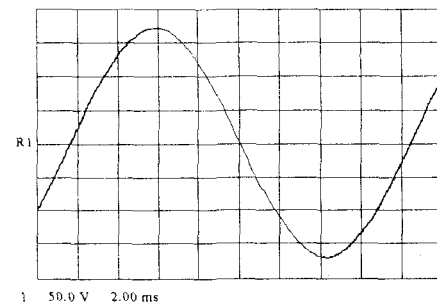


Fig. 15. Output voltage, unloaded inverter.

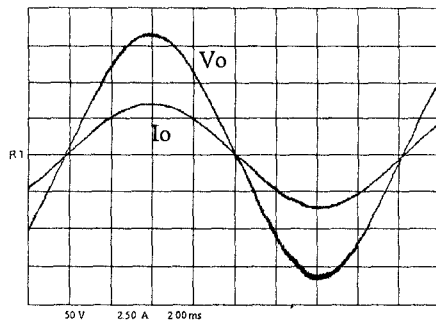


Fig. 16. Resistive load operation, $P_o = 250$ Watts.

V. CONCLUSIONS

Nowadays, it is very important to achieve high efficiency, low cost and high reliability in UPS design, and at the same time to fulfill the power quality standard (concerning PF and THD characteristics). This paper presents a novel approach in order to meet these objectives which is based on the reduction of the power conversion stages in both the battery charger and the inverter stages.

A boost inverter topology used in applications such as UPS is analyzed. This converter is different from the traditional inverter because it is able to boost and invert a signal at the same time. This converter requires a fast response, robustness and stability properties in order to reduce the distortion of the output voltage.

In order to show the performance of the designed controller, some simulation results have been made. It can be observed a good dynamics response, robustness and stability properties when the sliding mode based control has been applied.

Future work will be focused on finding another sliding surfaces that could be able to avoid the dependence of the dynamic response on the operating point.

REFERENCES

- [1] C. Aguilar, F. Canales, J. Arau, J. Sebastián and J. Uceda, "An Integrated Battery Charger/Discharger with Power Factor Correction", *IEEE Power Electronics Specialist Conference -PESC'95*, pp. 714 - 719.
- [2] R. Cáceres and Ivo Barbi, "A Boost DC - AC Converter: Operation, Analysis, Control and Experimentation", *Proceedings of International Conference on Industrial Electronics, Control and Instrumentation - IECON'95*, pp. 546 - 551.
- [3] R. Cáceres and Ivo Barbi, "A Boost DC - AC Converter: Principle of operation, Simulation and Implementation" (in Portuguese), *Proceedings of the Power Electronic Brazilian Congress -COBEP'95*, pp. 86 - 91.
- [4] R. Cáceres and Ivo Barbi, "Sliding Mode Controller for The Boost Inverter". *Proceedings of the IEEE International Power Electronics Congress -CIEP-96*, pp. 247 - 252.
- [5] R. Erickson, M. Madigan and S. Singer, "Design of a Simple High-Power-Factor Rectifier Based on the Flyback Converter", *IEEE Applied Power Electronics Conference -APEC '90*, pp. 792 - 801.
- [6] C. Aguilar, "Analysis of a Novel Scheme of an Integrated Battery Charger/Discharger with High Power Factor" (in Spanish), Ms. Sc. thesis, Centro Nacional de Investigación y Desarrollo Tecnológico (CENIDET), Cuernavaca, México, February 1995.
- [7] R. A. DeCarlo, S. Zak, G. P. Matthews, "Variable Structure Control of Nonlinear Multivariable Systems: A Tutorial", *Proceedings of the IEEE*, vol. 76 No. 3, March 1988, pp. 212 - 232.
- [8] J. Y. Hung, W. Gao, J. C. Hung, "Variable Structure Control: A Survey", *IEEE Transactions on industrial Electronics*, vol. 40, No. 1, Feb. 1993, pp. 2 - 18.
- [9] H. Sira-Ramírez, M. Ilic, "A Geometric Approach to the Feedback Control of Switch Mode dc-to-dc Power Supplies", *Transactions on circuits and systems*, vol. 35 No. 10, Oct. 1988, pp. 1291 - 1298.
- [10] P. Mattavelli, L. Rossetto, G. Spiazzi, "General purpose sliding mode controller for dc/dc converter applications", *IEEE Power Electronics Specialist Conference -PESC '93*, pp. 609 - 615.
- [11] M. Carpita, M. Marchesoni, "Experimental Study of a Power Conditioning Using Sliding Mode Control", *IEEE Transactions on power Electronics*, vol. 11 No. 5, Sept. 1996, pp. 731 - 742.
- [12] V. I. Utkin, "Sliding modes and their application in variable structure systems", *MIR Publishers*, Moscow, 1974.